

# bioETH-PRS: Confidential Polygenic Risk Scoring without a Trusted Evaluator via Fully Homomorphic Encryption on a Programmable Blockchain

Kimon Antonios Provas<sup>1,+,\*</sup>, Christos Galanopoulos<sup>1,+</sup>, Ilias Georgakopoulos-Soares<sup>1,\*</sup>

<sup>1</sup>Division of Pharmacology and Toxicology, College of Pharmacy, The University of Texas at Austin, Dell Pediatric Research Institute, Austin, TX, USA

<sup>+</sup>Co-first authors    <sup>\*</sup>Corresponding authors: [kap4722@my.utexas.edu](mailto:kap4722@my.utexas.edu); [ilias@austin.utexas.edu](mailto:ilias@austin.utexas.edu)

*Blockchain · Genomic Privacy · FHE · Smart Contracts · Privacy-Preserving Output Release*

## ABSTRACT

Polygenic risk scores (PRSs) aggregate genetic effect estimates to predict disease susceptibility, yet clinical deployment often exposes raw genotype data to third-party compute infrastructure. Prior homomorphic-encryption approaches, still require trust in a designated evaluator. We present **bioETH-PRS**, a protocol that replaces that evaluator role with immutable smart contracts on a blockchain supporting Fully Homomorphic Encryption (fhEVM). Using the integer-exact TFHE scheme, bioETH-PRS computes the PRS dot product entirely within the encrypted domain, keeping both genotype dosage vectors and GWAS weight vectors hidden from external parties throughout execution. We introduce a three-step fixed-point quantisation scheme for representing signed GWAS weights as unsigned 64-bit integers, achieving machine-epsilon reconstruction accuracy on validated fixtures. A four-contract architecture separates data custody, model publication, computation, and output release, and supports both a classic chunked path and a streaming path, with the latter reducing mock-measured gas by 37%. An on-chain noisy output oracle emits an encrypted noisy-score handle and a publicly decryptable ternary category, reducing raw score exposure and probing risk. Prototype evaluation on real GWAS fixtures confirms linear gas scaling and suggests that the approach may be cost-competitive in low-gas deployment environments.

## KEY POINTS

- bioETH-PRS replaces the trusted evaluator in encrypted PRS computation with auditable smart contracts on an FHE-enabled blockchain.
- The protocol protects both patient genotypes and GWAS model weights through encrypted execution and ACL-gated output release.
- A fixed-point quantisation scheme enables exact TFHE-compatible PRS computation with machine-epsilon reconstruction accuracy on validated fixtures.
- A streaming execution path reduces mock-measured

gas consumption by 37% relative to the classic chunked path.

- Anti-probing controls combine noisy output release with per-model, per-wallet, and per-sample rate limiting.

## 1 INTRODUCTION

Advances in genome sequencing have made polygenic risk scores (PRSs) a central tool in precision medicine [Wray et al., 2021, Inouye et al., 2018]. A PRS aggregates the dosage-weighted effects of genetic variants:

$$\text{PRS} = \sum_{i=1}^N g_i \cdot \beta_i, \quad (1)$$

where  $g_i \in \{0, 1, 2\}$  is the allele dosage of a genetic variant  $i$  and  $\beta_i$  is the corresponding GWAS effect weight. Published polygenic scores in the PGS Catalog range from small panels to genome-wide scores with large variant sets [Lambert et al., 2021], and hospital deployment increasingly involves transmitting raw genotype data to external compute infrastructure, a practice that raises acute privacy concerns given the re-identification risk of genomic sequences [Gymrek et al., 2013, Erlich and Narayanan, 2014].

**The double-privacy problem.** Two classes of sensitive information require simultaneous protection: (1) *patient genotypes* ( $g_i$ ), identifying, heritable, and permanent; and (2) *GWAS model weights* ( $\beta_i$ ), derived from restricted research cohorts. More generally, model interfaces and outputs can leak sensitive information through model-inversion attacks [Fredrikson et al., 2015]. Centralised cloud solutions protect neither of them, and both genotypes and weights must be decrypted before arithmetic can proceed.

**The FHE opportunity.** Fully Homomorphic Encryption (FHE) permits arbitrary arithmetic on encrypted data without decryption. Knight et al. [Knight et al., 2026] demonstrate this with HEPRS, an open-source pipeline that computes a 110,000-SNP schizophrenia PRS under the CKKS scheme [Cheon et al., 2017] with near-zero

# Trustless Confidential Polygenic Risk Scoring via FHE on Blockchain

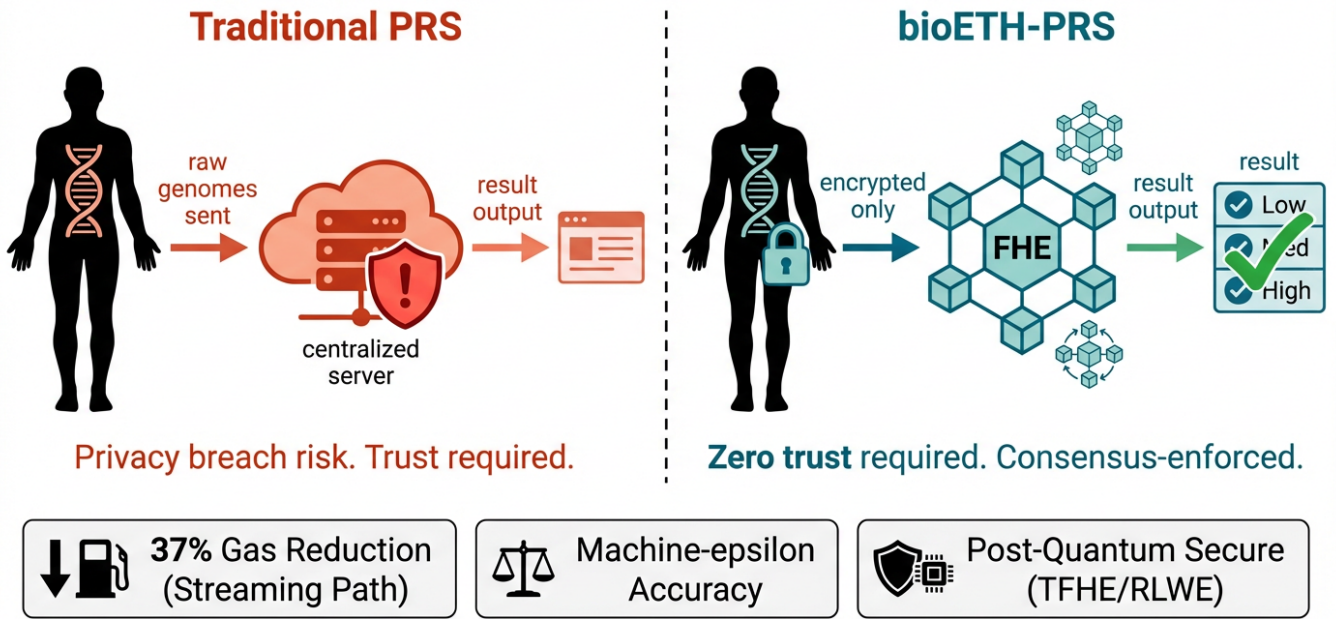


**Figure 1: Graphical Abstract.** bioETH-PRS replaces the trusted evaluator of conventional homomorphic PRS pipelines with consensus-enforced smart contracts. *Left:* Traditional centralised approaches transmit raw genotypes to a cloud evaluator, requiring user trust in a designated third party. *Right:* bioETH-PRS keeps all genomic data and model weights encrypted throughout, with computation verified by blockchain consensus. Key results: 37% gas reduction via streaming execution; machine-epsilon quantisation accuracy on real GWAS fixtures; post-quantum security under TFHE/RLWE.

accuracy loss ( $r > 0.999$ ,  $\text{MSE} < 2.3 \times 10^{-6}$ ). HEPRS, however, remains architecturally centralised: it relies on a three-party trust model (client, modeler, evaluator), and a colluding evaluator and client can reveal GWAS model weights. Trust in the evaluator is an assumption, not a protocol guarantee. Furthermore, HEPRS requires 3–4 GB of RAM per individual even at 110,000 SNPs, and output is a raw score—there is no built-in mechanism to prevent score accumulation or model probing.

**Our contribution.** We propose **bioETH-PRS**, which removes the designated evaluator of prior centralised FHE pipelines. On a blockchain augmented with an FHE coprocessor (fhEVM [Zama, 2024]), the evaluator is replaced by a deterministic, publicly auditable smart contract. This shifts trust from a single evaluator to auditable contract logic, blockchain consensus, the fhEVM coprocessor stack, and the ACL/ decryption infrastructure (Figure 1).

**Distinctions from HEPRS.** Although both systems compute the same encrypted PRS inner product, bioETH-PRS adds four design elements that are absent from HEPRS. First, TFHE/fhEVM exposes only unsigned integer arithmetic, requiring a dedicated fixed-point encoding and recovery scheme for signed GWAS weights; HEPRS instead uses CKKS with native approximate floating-point support. Second, bioETH-PRS separates data custody, model publication, computation, and output release into four independently auditable contracts with different trust and upgrade surfaces. Third, it introduces two fhEVM-specific execution strategies, classic and streaming, that

trade relay flexibility against gas and storage overhead under the handle/SSTORE model. Fourth, it restricts outputs through an oracle-enforced post-processing layer with anti-probing rate limits, rather than releasing raw scores directly.

Our main contributions are:

- A **four-contract architecture without a trusted evaluator** separating genomic data custody, model publication, computation, and post-processed output release—each independently auditable with distinct trust surfaces and upgrade lifecycles.
- A **three-step fixed-point quantisation scheme** bridging signed GWAS floats and unsigned TFHE integers with provable overflow safety and machine-epsilon reconstruction error, together with an automated advisor that selects the minimum viable scale factor before model publication.
- Two **gas-optimised execution strategies**: a classic chunked path enabling multi-party and relay-mediated computation, and a streaming path with 37% gas reduction for single-requester flows.
- An **on-chain noisy output oracle** with cryptographically generated noise, mandatory oracle-required enforcement, and minimum threshold-gap constraints that together reduce score probing risk and prevent raw-score bypass.
- A **rate-limiting mechanism** based on per-model, per-

wallet, and per-sample, block-windowed job quotas that raise the cost of model weight extraction to thousands of hours at recommended settings.

- Prototype evaluation on real HEPRS GWAS fixtures (100–5,000 SNPs) confirming linear gas scaling, exact score correctness, and economically plausible analysis costs under L2-equivalent gas pricing assumptions.

## 2 BACKGROUND

### 2.1 Polygenic Risk Scores

A PRS is the weighted inner product of a patient’s genotype dosage vector  $\mathbf{g} \in \{0, 1, 2\}^N$  and a GWAS effect weight vector  $\boldsymbol{\beta} \in \mathbb{R}^N$  (Eq. 1). Effect weights are typically estimated by large-scale GWAS over tens of thousands of individuals and are signed floating-point values in the range  $[-0.5, +0.5]$ . Standard pipelines such as PLINK 2 [Chang et al., 2015] and LDpred2 [Privé et al., 2020] compute PRSs in milliseconds on plaintext data; FHE approaches trade runtime for privacy.

PRS models span a wide range in SNP inclusion depending on construction methodology. Sparse or clinically oriented models may include hundreds to a few thousand variants, while genome-wide approaches incorporate tens of thousands to millions of SNPs. In this work, we perform a proof of principle study with 5,000 SNPs, with on-chain FHE computation.

The computation in Eq. 1 is an inner product between two vectors of moderate length. This is exactly the primitive that FHE systems are designed to support efficiently, making PRS computation a natural target for FHE-based privacy enhancement.

### 2.2 Fully Homomorphic Encryption

FHE schemes differ in the arithmetic they support and their performance. Two are directly relevant to this work.

**CKKS** [Cheon et al., 2017] supports approximate arithmetic over real-valued data, is naturally suited to floating-point computations, and underpins HEPRS. It allows arbitrary depth computation at the cost of accumulating approximation error. The Lattigo library [Tune Insight SA, 2022] implements CKKS in Go with the parameter sets used by HEPRS. CKKS is computationally expensive: evaluating a 110,000-SNP PRS on a single CPU node requires approximately 4.9 s per individual and up to 130 GB of RAM for a cohort of 1,000 [Knight et al., 2026].

**TFHE** [Chillotti et al., 2020] operates on exact unsigned integers and supports bootstrapping to arbitrary computation depth. Zama’s fhEVM implements TFHE as EVM precompile operations exposed to smart contracts. TFHE provides deterministic integer arithmetic, a better fit for smart contracts where bit-exact reproducibility is required for consensus. The cost is that signed floating-point weights must be converted to unsigned integer encodings, motivating our quantisation design (Section 4).

TFHE security is grounded in the Ring Learning with Errors (RLWE) hardness assumption [Chillotti et al., 2020], which is believed to be quantum-resistant. CKKS under the RLWE assumption likewise provides post-quantum security. Both are therefore appropriate choices for long-term genomic data protection.

### 2.3 Programmable Blockchain and fhEVM

The Fully Homomorphic Ethereum Virtual Machine (fhEVM) extends the Ethereum execution environment with TFHE precompile operations [Zama, 2024]. Every encrypted value is represented on-chain by a 32-byte opaque handle; actual ciphertexts are managed by an off-chain coprocessor. Smart contracts store only handles and trigger FHE operations through coprocessor calls.

Access to encrypted outputs is governed by an on-chain ACL contract: a handle is decryptable only by addresses explicitly granted access by the ACL. The blockchain is the trust anchor—no party can obtain a decryption unless the executing smart contract grants it, and the smart contract’s grant conditions are publicly auditable.

A per-transaction Homomorphic Computation Unit (HCU) budget limits the number of FHE operations per block. In our Ethereum mock-coprocessor prototype, we measured a budget of 60–74 FHE operations per transaction (Section 7); the Sepolia testnet ceiling is expected to be higher but remains to be measured. The HCU constraint necessitates chunked computation strategies for large input vectors.

## 3 SYSTEM DESIGN

### 3.1 Architecture Overview

bioETH-PRS is structured as four independently deployable smart contracts forming a linear pipeline from sample data custody to risk output (Figure 2). The four-layer separation reflects distinct trust surfaces and upgrade lifecycles: the data registry protects patient data; the marketplace protects researcher GWAS models; the compute engine implements computation logic; the oracle enforces privacy policy. Each contract is independently auditable and can be replaced without affecting the others.

**Genomic Registry.** URI-based registry of sample datasets with per-address access control lists (ACLs). Stores references (IPFS or Arweave URIs) to off-chain encrypted genotype data. A patient registers samples and explicitly grants compute access to specific callers. This contract performs no FHE operations; it is a lightweight permission layer.

**Model Marketplace.** Immutable repository of GWAS weight vectors published in chunks. Weights may be stored as plaintext integers (public models, enabling a cheaper coprocessor-optimised ciphertext-times-plaintext multiply,  $\approx 60\%$  less expensive than ciphertext-ciphertext) or as encrypted handles (private models). A manifest

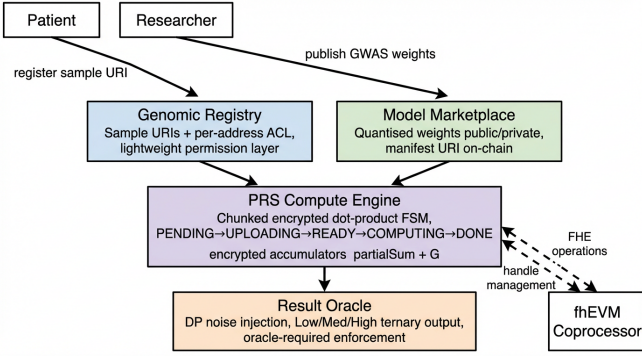


**Figure 2:** System architecture. Four on-chain smart contracts form a linear pipeline from genomic data custody to privacy-preserving risk output. The fhEVM coprocessor manages off-chain ciphertexts; only opaque 32-byte handles are stored on-chain. No plaintext genotype data or model weights are observable at any stage.

URI records quantisation metadata on-chain: scale factor, weight zero-point, score offset, and provenance hash. Models are immutable after finalisation; version management is the responsibility of the publishing researcher.

**PRS Compute Engine.** The core computation contract. Implements a finite state machine (PENDING → UPLOADING → READY → COMPUTING → DONE) that orchestrates chunked dot-product accumulation of patient SNPs against model weights. The engine tracks two encrypted running accumulators: the weighted partial sum and the genotype sum (required for quantisation correction; see Section 4). Final score handles are ACL-granted only to the requesting party. Two parallel execution paths are supported (Section 5).

**Result Oracle.** Applies on-chain cryptographic noise and emits an encrypted noisy score handle plus a publicly decryptable ternary risk category. Noise is generated by the fhEVM’s on-chain random source, making it unknowable to any party before the transaction is mined. The oracle can be set as mandatory by the model owner, preventing direct requester access to the raw score when oracle-required mode is enabled.

### 3.2 Comparison with HEPRS

Table 1 summarises the key architectural differences between bioETH-PRS and HEPRS [Knight et al., 2026]. HEPRS achieves near-perfect accuracy on a 110,000-SNP schizophrenia model running on commodity hardware, but its three-party trust assumption means a colluding evaluator and client can reveal model weights. bioETH-PRS removes the designated evaluator assumption by replacing that role with auditable on-chain code.

The core mathematical operation is identical in both systems: the PRS dot product of Eq. 1. The critical difference is in the trust model and the FHE scheme. CKKS handles signed floats natively; TFHE requires unsigned integer encoding. CKKS evaluates approximate arithmetic; TFHE arithmetic is exact. The evaluator-free architecture of

bioETH-PRS comes at the cost of restricting the practical SNP range to 100–5,000—a regime that captures a subset of curated PRS models [Lambert et al., 2021] while remaining feasible for on-chain computation.

**Table 1:** Architectural comparison: HEPRS vs. bioETH-PRS

Property	HEPRS [Knight et al., 2026]	bioETH-PRS
FHE scheme	CKKS (approx. floats)	TFHE (exact integers)
Evaluator	Centralised server	Smart contract
Trust model	3-party non-collusion	Evaluator removed; consensus/fhEVM dependent
Weight privacy	Evaluator-gated	ACL-gated, immutable
Output control	External (optional)	On-chain noisy release
GWAS weight type	Signed floats	Quant. uint64
Max variants tested	110,000	5,000 (scalable)
Per-person latency	~4.9 s	~386 ms (100 SNPs)
Score access	By client	Noisy score + category
Post-quantum	Yes (CKKS/RLWE)	Yes (TFHE/RLWE)

## 4 QUANTISATION SCHEME

### 4.1 The Representation Problem

TFHE arithmetic on the fhEVM operates on unsigned 64-bit integers. GWAS weights  $\beta_i$  are signed floating-point values; a naive fixed-point encoding that multiplies by a scale factor  $s$  and rounds produces quantised weights  $q_i = \text{round}(s \cdot \beta_i) \in \mathbb{Z}$ , which may be negative. Negative integers cannot be stored in an unsigned 64-bit integer and would silently wrap under modular overflow, corrupting results without any observable error. A correct encoding must guarantee that all intermediate encrypted values remain in the non-negative range  $[0, 2^{64} - 1]$  for any genomically valid input  $g_i \in \{0, 1, 2\}$ .

### 4.2 Three-Step Unsigned Encoding

We address this with a three-step bijection that maps the space of signed floating-point dot products into a guaranteed non-negative 64-bit integer range (Figure 3).

**Step 1: Scale.**

$$q_i = \text{round}(s \cdot \beta_i), \quad q_i \in \mathbb{Z}, \quad (2)$$

where  $s$  is a model-specific scale factor selected by an automated quantisation advisor (Section 4.5).

**Step 2: Weight zero-point shift.** Let

$$z_w = -\min_i q_i, \quad u_i = q_i + z_w \geq 0 \quad \forall i. \quad (3)$$

The shifted weights  $u_i \geq 0$  are stored on-chain. The raw accumulation  $\sum_i g_i u_i$  overestimates the true PRS by the constant  $z_w \cdot \sum_i g_i$ , requiring correction. The engine tracks the genotype sum  $G = \sum_i g_i$  as a second encrypted accumulator to enable this correction.

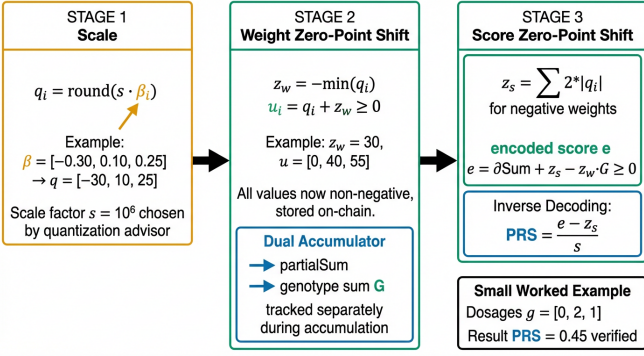


**Figure 3:** Three-step fixed-point quantisation scheme. Signed GWAS floats are (1) scaled by  $s$ , (2) shifted by the weight zero-point  $z_w$  to guarantee non-negative weights, and (3) shifted by the score zero-point  $z_s$  to guarantee a non-negative encoded score. Decoding inverts all three steps after decryption.

**Step 3: Score zero-point shift.** Even after the weight correction, the corrected sum  $P = \sum_i g_i u_i - z_w G$  can be negative for patients with many risk-decreasing alleles. We define:

$$z_s = - \sum_{i:\beta_i < 0} 2q_i = \sum_{i:\beta_i < 0} 2|q_i|, \quad (4)$$

$$e = P + z_s \geq 0. \quad (5)$$

$e$  is the *encoded score* stored encrypted on-chain. The on-chain computation is structured to avoid any intermediate negative value:

$$e = (\text{partialSum} + z_s) - (z_w \cdot G), \quad (6)$$

where  $z_s$  is added before subtracting  $z_w G$ , ensuring the intermediate value ( $\text{partialSum} + z_s$ ) is always non-negative.

**Decoding.** After decryption by the authorised requester:

$$\text{PRS} = \frac{e - z_s}{s}. \quad (7)$$

### 4.3 Worked Example

Consider 3 genetic variants with weights  $\beta = [-0.30, 0.10, 0.25]$ , scale  $s = 100$ , and dosages  $\mathbf{g} = [0, 2, 1]$ .

1. Quantise:  $\mathbf{q} = [-30, 10, 25]$ .
2. Weight shift:  $z_w = 30$ ,  $\mathbf{u} = [0, 40, 55]$ .
3. Accumulate:  $\text{partialSum} = 0 \cdot 0 + 2 \cdot 40 + 1 \cdot 55 = 135$ ;  
 $G = 0 + 2 + 1 = 3$ .
4. Correction:  $P = 135 - 30 \cdot 3 = 45$ .
5. Score shift:  $z_s = 2 \cdot 30 = 60$ ;  $e = 45 + 60 = 105$ .
6. Decode:  $\text{PRS} = (105 - 60)/100 = 0.45$ .
7. Verify: plaintext  $\text{PRS} = 0 \cdot (-0.30) + 2 \cdot 0.10 + 1 \cdot 0.25 = 0.45$ . ✓

### 4.4 Overflow Safety

**Proposition 1.** Let  $N$  be an arbitrary SNP count, let  $s$  be the fixed-point scale factor, and let  $M$  satisfy  $|q_i| \leq sM$

for every quantised weight  $q_i$ . Then a sufficient worst-case condition for unsigned 64-bit safety of the full encoding pipeline is

$$4sMN \leq 2^{64} - 1.$$

Equivalently,

$$N \leq \left\lfloor \frac{2^{64} - 1}{4sM} \right\rfloor.$$

Under this condition, both the final encoded score  $e$  and the intermediate quantity withOffset = partialSum +  $z_s$  in Eq. 6 fit in `uint64`.

*Proof.* Partition the quantised weights into positive, negative, and zero sets with cardinalities  $N_+$ ,  $N_-$ , and  $N_0$ , so that  $N_+ + N_- + N_0 = N$ . Because  $g_i \in \{0, 1, 2\}$  and  $z_w = -\min_i q_i \leq sM$ , the shifted weight  $u_i = q_i + z_w$  obeys

$$u_i \leq \begin{cases} 2sM, & q_i > 0, \\ sM, & q_i \leq 0. \end{cases}$$

Hence the encrypted accumulation before correction satisfies

$$\text{partialSum} = \sum_i g_i u_i \leq 4sMN_+ + 2sM(N_- + N_0).$$

The score zero-point satisfies

$$z_s = - \sum_{i:q_i < 0} 2q_i \leq 2sMN_-.$$

Therefore the intermediate value materialised in Eq. 6 is bounded by

$$\text{withOffset} = \text{partialSum} + z_s \leq 4sMN_+ + 4sMN_- + 2sMN_0 \leq 4sMN$$

This is the binding worst-case accumulator bound.

For the final encoded score, observe that the weight-shift correction exactly cancels the zero-point contribution:

$$P = \text{partialSum} - z_w G = \sum_i g_i q_i.$$

Thus

$$-2sMN_- \leq P \leq 2sMN_+,$$

and after adding  $z_s$  we obtain

$$0 \leq e = P + z_s \leq 2sM(N_+ + N_-) \leq 2sMN.$$

So the encoded score range itself fits in `uint64` under the weaker bound  $2sMN \leq 2^{64} - 1$ , but the actual implementation must also accommodate the larger intermediate withOffset. Therefore the sufficient adversarial safety condition for all intermediate and final values is

$$4sMN \leq 2^{64} - 1.$$

For example, at the balanced scale  $s = 10^6$  with  $M = 1$ , this yields the mathematical worst-case ceiling

$$N \leq \left\lfloor \frac{2^{64} - 1}{4 \times 10^6} \right\rfloor \approx 4.61 \times 10^{12},$$

which is many orders of magnitude above the fixture sizes used in our prototype evaluation.

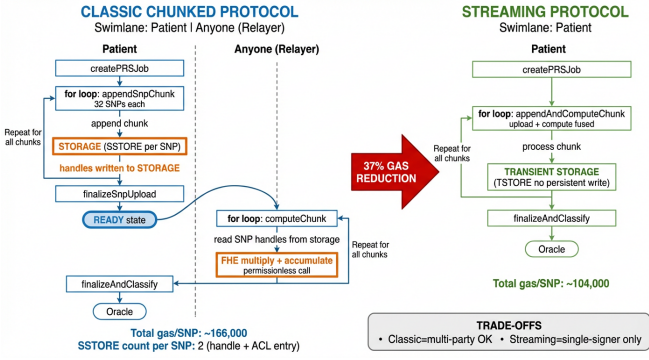


**Figure 4:** Execution protocol comparison. The classic chunked path persists SNP handles in contract storage (SSTORE), enabling multi-party upload/compute separation. The streaming path uses EIP-1153 transient storage (TSTORE), eliminating two SSTORE operations per SNP and reducing total gas by 37%. Both paths finalize through the Result Oracle.

#### 4.5 Quantisation Advisor

Before publishing any model, an automated quantisation advisor evaluates candidate scale values  $s \in \{10^2, 10^4, 10^6, 10^8, 10^{10}\}$  against the actual GWAS weight distribution. For each  $s$ , the advisor computes the mean absolute error (MAE) between the quantised dot product and the floating-point PRS for all individuals in the fixture. It outputs a recommendation from three tiers:

- **Baseline** ( $s \approx 10^2$ ): 1–15% MAE. Proof-of-concept only.
- **Balanced** ( $s \approx 10^6$ ): machine-epsilon error. Recommended default for all production models.
- **Max precision** ( $s \approx 10^8$ ): no improvement over balanced on real GWAS fixtures; the limiting factor is source data precision.

The advisor runs in  $\approx 200$  ms and should be executed before every model publication. Gas cost is unaffected by scale choice—the bottleneck is SNP upload transaction count, not arithmetic precision.

## 5 EXECUTION PROTOCOLS

bioETH-PRS provides two computation strategies that differ in their gas cost, storage semantics, and support for multi-party participation (Figure 4). Both strategies produce bit-identical results.

### 5.1 Classic Chunked Protocol

The classic protocol separates SNP ingestion from computation, enabling different parties to execute different phases at different times.

The upload chunk size  $r_u \leq 32$  is constrained by the fhEVM input-proof budget (2048 bits / 64 bits per encrypted integer). The compute chunk size  $r_c \leq 20$  is constrained by the HCU budget: each compute chunk

### Algorithm 1 Classic chunked PRS computation (patient and relayer)

- 1: **Patient:** CREATEPRSJOB(modelId, sampleId)  $\triangleright$  ACL checked; model geometry loaded
- 2: **for**  $k \leftarrow 0$  to  $\lceil N/r_u \rceil - 1$  **do**
- 3:   **Patient:** APPENDSNPCHUNK(jobId, encSNPs $_k$ , proof)  $\triangleright \leq r_u = 32$  SNPs; handles persisted
- 4: **end for**
- 5: **Patient:** FINALIZESNPUPLOAD(jobId)  $\triangleright$  Job transitions to READY
- 6: **for**  $k \leftarrow 0$  to  $\lceil N/r_c \rceil - 1$  **do**
- 7:   **Anyone:** COMPUTECHUNK(jobId)  $\triangleright$  Permissionless; reads persisted SNP handles
- 8:     partialSum +=  $\sum_{i \in \text{chunk}} g_i \cdot u_i$
- 9:      $G$  +=  $\sum_{i \in \text{chunk}} g_i$
- 10: **end for**
- 11: **Patient:** FINALIZEANDCLASSIFY(jobId, oracle,  $\tau_L$ ,  $\tau_H$ )

### Algorithm 2 Streaming PRS computation (patient, single-signer flow)

- 1: **Patient:** CREATEPRSJOB(modelId, sampleId)
- 2: **for**  $k \leftarrow 0$  to  $\lceil N/r_c \rceil - 1$  **do**
- 3:   **Patient:** append chunk encSNPs $_k$  with proof  $\triangleright r_c$  SNPs; handles transient only
- 4:     partialSum +=  $\sum_{i \in \text{chunk}} g_i \cdot u_i$
- 5:      $G$  +=  $\sum_{i \in \text{chunk}} g_i$   $\triangleright$  SNP handles discarded after each call
- 6: **end for**
- 7: **Patient:** FINALIZEANDCLASSIFY(jobId, oracle,  $\tau_L$ ,  $\tau_H$ )

of  $r_c$  SNPs executes  $3r_c + 2$  FHE operations (multiply, accumulate partial sum, accumulate genotype sum per SNP, plus two coprocessor calls for accumulator handles). At  $r_c = 20$  this yields 62 operations—within the measured HCU budget.

SNP ciphertext handles are persisted in a flat per-job mapping across transactions, enabling upload and compute to be executed by different parties or at different times. The **compute phase is permissionless**: any third party may advance computation by calling the compute function. Because computation is deterministic and non-interactive, a relayer learns no plaintext information and cannot affect correctness or confidentiality.

### 5.2 Streaming Protocol

The streaming protocol fuses upload and computation into a single call per chunk (Algorithm 2). Each call validates the incoming SNP handles using EIP-1153 transient storage (scoped to the current transaction), immediately multiplies them against model weights, accumulates the results, and discards the handles. No per-SNP persistent storage writes are performed.

**Gas savings.** The classic path requires two persistent storage writes per SNP: a handle record in contract storage and an ACL entry—each an Ethereum SSTORE at approximately 25,000 gas. The streaming path eliminates both, saving  $\approx 50,000$  gas per SNP, which accounts for the observed 37% total reduction. The irreducible cost

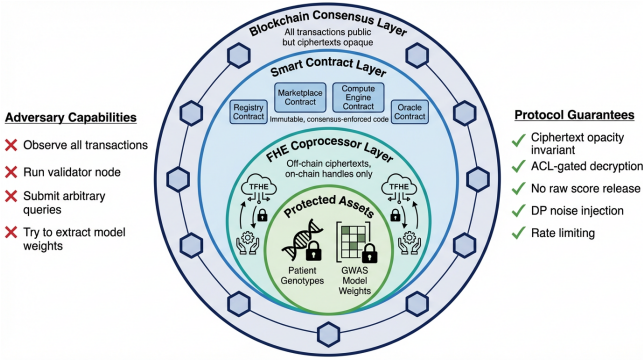


**Figure 5:** Security threat model and defence layers. The TFHE/RLWE hardness assumption grounds the innermost layer. Successive layers—FHE coprocessor, smart contracts, blockchain consensus—add verifiable security properties. Adversary capabilities and corresponding protocol guarantees are enumerated at the threat-boundary interface.

floor of  $\approx 95,000$ – $104,000$  gas/SNP comprises the input-proof verification, FHE multiply, and FHE accumulate—coprocessor-level costs not reducible by contract design.

**Trade-off.** The streaming path is incompatible with multi-party upload/compute separation: upload and compute are coupled within the same transaction, restricting execution to a single signer. The classic path remains the appropriate choice for relay services and architectures where upload and compute are performed by different parties.

## 6 SECURITY MODEL

### 6.1 Threat Model

We consider a computationally bounded adversary with full network access to the blockchain and coprocessor (Figure 5). The adversary may: observe all on-chain transactions and storage slots; operate a validator node and read all encrypted handles; submit arbitrary transactions; and query classification outputs repeatedly with chosen SNP inputs. The adversary may not break the TFHE hardness assumption (grounded in the RLWE problem) or forge ACL entries.

### 6.2 Core Privacy Invariants

We formalise the protocol’s privacy guarantees as five critical invariants:

**Invariant 1** (Ciphertext opacity). *Encrypted handles are 32-byte opaque identifiers; raw ciphertexts reside exclusively at the off-chain coprocessor. No on-chain party stores or observes plaintexts at any point during computation.*

**Invariant 2** (ACL-gated decryption). *Every encrypted output is associated with an ACL record. Decryption requires an explicit ACL grant that can only be issued by the executing smart contract upon satisfying the protocol’s state-machine preconditions.*

**Invariant 3** (No raw score release). *The final encoded PRS  $e$  (Eq. 6) is never made publicly decryptable. When oracle-required mode is disabled, the requester may obtain ACL-gated decryption access to the raw score through `finalize()`. When oracle-required mode is enabled, that requester path is disabled: the raw score handle is routed only to the approved oracle, while the Result Oracle emits an encrypted noisy score handle and a publicly decryptable ternary category after noise addition.*

**Invariant 4** (Oracle-required mode). *A model owner may set an oracle-required flag, causing the compute engine to revert on any attempt to release the raw score handle directly to the requester without passing through the noisy output oracle. This prevents requesters from bypassing noise by decrypting raw scores. When oracle-required mode is active, only the registered approved oracle address may receive the encrypted raw-score handle.*

**Invariant 5** (Single-finalize guarantee). *Each compute job carries a finalized flag. Any finalization path sets this flag and reverts on subsequent calls, preventing a requester from obtaining multiple score handles for a single rate-limit slot.*

### 6.3 Noisy Output Release

The current Result Oracle implements a DP-inspired noisy output release mechanism, not a formally calibrated  $(\epsilon, \delta)$ -differential privacy guarantee. For each classification request, noise is drawn from  $[0, B)$  where  $B$  is a power-of-two immutable constant set at oracle deployment:

$$e_{\text{noisy}} = e + \nu, \quad \nu \sim \text{Uniform}(0, B). \quad (8)$$

The noise  $\nu$  is generated by the fhEVM random source, unseeded by the caller and determined solely by block randomness. The caller has no influence over  $\nu$ .

All comparisons against classification thresholds operate on the noisy encrypted score using encrypted boolean operations, avoiding any branching on hidden values:

$$\begin{aligned} \hat{L} &= \mathbb{K}[e_{\text{noisy}} < \tau_L], \\ \hat{H} &= \mathbb{K}[e_{\text{noisy}} \geq \tau_H], \\ \text{cat} &= \text{select}(\hat{L}, L, \text{select}(\neg \hat{L} \wedge \neg \hat{H}, M, H)). \end{aligned} \quad (9)$$

The encrypted select primitive replaces conditional branching, preventing side-channel leakage of the comparison result. The minimum threshold-gap requirement  $\tau_H - \tau_L \geq B$  ensures the noisy score cannot deterministically map to a single category regardless of  $e$ , reducing straightforward threshold-probing strategies.

**Interpretation and limits.** This mechanism is best understood as an anti-probing control that randomises the released classification boundary. A formal DP claim would require an explicit neighbouring-dataset definition, a sensitivity analysis for the PRS score under the chosen adjacency relation, and calibration of  $B$  to concrete privacy parameters. Those steps are not yet part of the

present prototype, so we avoid assigning specific  $(\epsilon, \delta)$  values.

**Bias correction.** Uniform noise on  $[0, B)$  introduces an expected upward bias of  $B/2$ . Callers must adjust classification thresholds by this amount, a deterministic correctable offset exposed by the oracle’s view function. The anti-probing effect derives from noise variance, not its mean.

### 6.4 Anti-Probing: Rate Limiting

Without query limits, an adversary could mount a model-extraction attack by submitting many classification queries with crafted SNP inputs and observing the resulting categories. The compute engine enforces per-model, per-wallet, and per-sample block-windowed job quotas to raise this cost.

Let  $R$  be the maximum queries per  $W$ -block window,  $B$  the noise bound, and  $K = 3$  the number of output categories. Each query reveals at most  $\log_2(K) \approx 1.58$  bits minus noise entropy. At suggested settings for private models ( $R = 3, W = 1000, B = 128$ ), extracting a single 20-bit weight requires approximately  $2 \times 10^4 / (3 \times 1.58) \approx 4,220$  block windows, corresponding to  $\approx 2,800$  hours at 12 s/block. Block-based windows (rather than timestamps) prevent miner manipulation of window boundaries.

## 7 EMPIRICAL EVALUATION

### 7.1 Experimental Setup

**Prototype evaluation (mock coprocessor).** We evaluate bioETH-PRS against the four fixture sizes (100, 500, 1,000, and 5,000 SNPs) from the HEPRS reference dataset [Knight et al., 2026], which contains real GWAS beta weights for a schizophrenia model at each size. Gas measurements use a Hardhat in-process mock coprocessor that validates the complete fhEVM protocol (handles, ACL, input proofs) while performing plaintext arithmetic; gas numbers are expected to be within 10–20% of real-network deployment. The HCU ceiling was measured empirically: chunk sizes of 20 SNPs (62 ops) pass; 25 SNPs (77 ops) fail, confirming the measured 60–74-operation HCU budget. All experiments use upload chunk size  $r_u = 32$  and compute chunk size  $r_c = 20$ .

### 7.2 Quantisation Accuracy

At the balanced scale tier ( $s \approx 10^6$ ), reconstructed PRSs agree with floating-point computation to machine epsilon across all 50 individuals in each of the four fixtures (200 individual-fixture combinations), as shown in Table 2. No negative encoded scores or unsigned 64-bit integer overflow events were observed. The baseline tier ( $s \approx 10^2$ ) yielded 1–15% MAE—unsuitable for clinical use, as a 15% score error is equivalent to misclassifying borderline patients. The max-precision tier ( $s \approx 10^8$ ) provided no

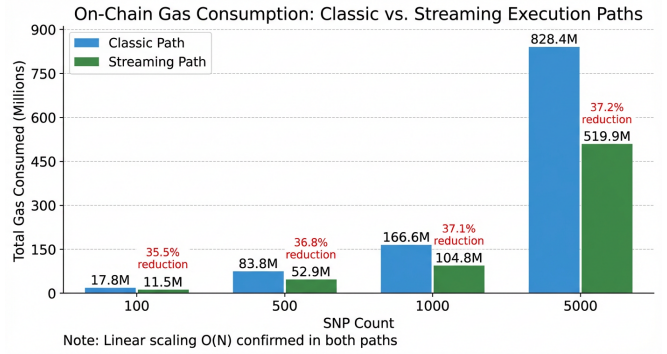


**Figure 6:** On-chain gas consumption versus SNP count for both execution paths. Gas scales linearly ( $\mathcal{O}(N)$ ) in both cases. The streaming path achieves 35.5–37.2% gas reduction over the classic chunked path by eliminating persistent SSTORE operations for intermediate SNP ciphertext handles.

additional accuracy improvement: the limiting factor is the number of significant digits in the source GWAS betas rather than the encoding resolution. This confirms that the balanced tier ( $s \approx 10^6$ ) is both necessary and sufficient for production deployment.

**Table 2:** Quantisation accuracy on HEPRS fixtures (balanced tier)

SNPs	Scale $s$	Bits req.	MAE	Indiv.
100	$3 \times 10^6$	16	$< \epsilon_{\text{mach}}$	50/50 pass
500	$3 \times 10^6$	16	$< \epsilon_{\text{mach}}$	50/50 pass
1,000	$1 \times 10^6$	16	$< \epsilon_{\text{mach}}$	50/50 pass
5,000	$1 \times 10^6$	16	$< \epsilon_{\text{mach}}$	50/50 pass

### 7.3 Gas Consumption and Scaling

Figure 6 and Table 3 report total gas consumption across execution paths and fixture sizes in the mock-coprocessor prototype environment. Gas scales linearly with SNP count in both paths, confirming the absence of hidden quadratic overhead at the contract layer. The streaming path saves approximately 37% above 500 SNPs, driven entirely by the elimination of two SSTORE operations per SNP.

**Table 3:** Mock-environment total gas consumption by execution path

SNPs	Classic	Streaming	Reduction
100	17,822,364	11,496,911	35.5%
500	83,943,764	53,021,675	36.8%
1,000	166,832,473	104,972,012	37.1%
5,000	829,373,084	520,440,311	37.2%

### 7.4 Per-SNP Cost Decomposition

Table 4 decomposes per-SNP gas. The irreducible floor of  $\approx 95,000$ – $104,000$  gas/SNP comprises the input-proof verification, FHE multiply, and FHE accumulate—operations

set by the fhEVM protocol and not reducible by contract design choices. Future improvements in coprocessor throughput or lighter-weight proof schemes would directly reduce this floor.

**Table 4:** Per-SNP gas decomposition

Operation	Classic	Streaming
Input proof verification	~50,000	~50,000
FHE multiply	~27,000	~27,000
FHE accumulate (partial sum)	~27,000	~27,000
Handle SSTORE (classic only)	~25,000	—
ACL SSTORE (classic only)	~25,000	—
SLOAD, misc. overhead	~12,000	—
<b>Total/SNP</b>	<b>~166,000</b>	<b>~104,000</b>

### 7.5 Latency

On the Hardhat mock coprocessor, end-to-end wall-clock times for the streaming path are: 100 SNPs: ~386 ms; 500 SNPs: ~1.5 s; 1,000 SNPs: ~2.8 s; 5,000 SNPs: ~14.5 s. These are local simulation timings; real-network latency is dominated by per-block confirmation time, as each chunk corresponds to one on-chain transaction. The transaction count scales as  $\lceil N/r_c \rceil + 2$  for the streaming path.

### 7.6 Deployment Cost Projections

Table 5 projects per-analysis cost across three gas pricing scenarios. These figures are scenario analyses derived from mock-environment gas measurements, not measured deployment prices. Ethereum L1 pricing (30 gwei) renders the system economically unviable for clinical use. At L2-equivalent pricing on a purpose-built FHE rollup (0.05 gwei), 100-SNP and 500-SNP analyses project to \$1.72 and \$7.95, respectively. Under such low-gas assumptions, the system may become cost-competitive with centralised commercial genomics services (\$50–\$300), but that comparison remains contingent on real-network deployment. Dedicated application-chain deployment reduces costs by two further orders of magnitude in the same pricing model, making even 5,000-SNP analyses economically plausible at \$1.56 per run.

**Table 5:** Projected USD cost per analysis (streaming path, ETH at \$3,000)

SNPs	L1 (30 gwei)	L2 (0.05 gwei)	Appchain
100	\$1,035	\$1.72	\$0.034
500	\$4,772	\$7.95	\$0.159
1,000	\$9,447	\$15.75	\$0.315
5,000	\$46,840	\$78.07	\$1.561

### 7.7 Correctness and Protocol Verification

For each fixture size, we verified that the on-chain encoded score, after decryption and application of the quantisation inverse mapping, matches the plaintext floating-point dot

product. For the 100-SNP HEPRS fixture, the expected encoded score of 758,685 was reproduced exactly across all validation runs. Both execution paths produce identical scores for all four fixture sizes (verified with plaintext arithmetic in the mock coprocessor).

Protocol invariants—ACL enforcement, state-machine integrity, single-finalize guarantee, minimum threshold gap, oracle-required mode, approved-oracle enforcement, rate-limiting window behaviour, and ACL revocation handling—were validated across 134 automated test cases. The HCU ceiling probe confirmed the mock budget at 60–74 operations per transaction.

## 8 ACCESS CONTROL AND COMPUTE FLOWS

### 8.1 Encrypted Handle Lifecycle

Every encrypted value in the fhEVM has an associated ACL record maintained in a dedicated on-chain contract. The ACL maps handles to authorised addresses and distinguishes four grant types with different persistence semantics:

- **Persistent contract grant:** Written to the ACL contract’s persistent storage via SSTORE. Allows the owning contract to use the handle in future transactions. This is the primary source of gas cost in the classic upload path (~25,000 gas per SNP handle).
- **Persistent user grant:** Written to the ACL contract via SSTORE. Allows an end-user to decrypt the handle via the KMS gateway. Applied at finalization to grant the requester access to their encoded score.
- **Transient grant:** Uses EIP-1153 transient storage. Valid only for the current transaction. The streaming path relies exclusively on transient grants for intermediate SNP handles, avoiding the SSTORE cost entirely.
- **Public grant:** Enables anyone to decrypt. Applied only to the ternary risk category after noise addition; never applied to score values.

The ACL design is the root of the 37% gas differential between the classic and streaming paths. In the classic path, each of the  $N$  SNP handles requires a persistent contract grant (SSTORE in the ACL) and a handle write to contract storage (second SSTORE). In the streaming path, transient grants are used for SNP handles and the SSTORE costs are eliminated.

### 8.2 State Machine and Mutual Exclusion

The PRS Compute Engine enforces a strict job state machine to prevent incorrect ordering of operations:

PENDING → UPLOADING → READY → COMPUTING → DONE.

The classic and streaming paths are mutually exclusive per job. The guard condition uses upload counts: if any

SNP handles have been written to persistent storage, the classic path is in use and streaming calls are rejected; if computation has advanced without persistent uploads, the streaming path is in use. This prevents hybrid calls that could compromise the handle-lifecycle invariants.

### 8.3 Private Model Access Control

When a GWAS model is published with private (encrypted) weights, access control is layered: the model owner must first authorise the compute engine as a reader; individual requesters must also be added to the private model reader list; and each compute chunk re-checks reader authorisation, so revocation of a requester mid-job causes the next compute chunk to fail, effectively terminating the job. This is in contrast to the registry ACL, which is checked only at job creation. The asymmetric behaviour between registry and model ACL is documented and empirically verified.

## 9 DISCUSSION

Our work presents bioETH-PRS, a privacy-preserving framework for polygenic risk scoring that replaces the trusted third-party evaluator used in prior homomorphic-encryption approaches with auditable smart contracts on an FHE-enabled blockchain. It enables encrypted computation of PRS while protecting both patient genotypes and GWAS model weights, introduces an overflow-safe quantization scheme, and demonstrates linear scaling, exact score correctness, and a 37

### 9.1 HEPRS and bioETH-PRS: Complementary Systems

bioETH-PRS and HEPRS [Knight et al., 2026] are best understood as complementary rather than competing systems occupying different points in a design space defined by trust requirements and scalability.

HEPRS is appropriate when: (1) three-party non-collusion can be organisationally enforced (e.g., hospital evaluator, academic modeler, clinical client); (2) SNP counts exceed 5,000; and (3) the evaluation environment provides sufficient RAM (>65 GB for 1,000 individuals at 110,000 SNPs). In this context, CKKS’s native signed float arithmetic eliminates the need for quantisation.

bioETH-PRS is appropriate when: (1) no trusted evaluator can be assumed; (2) model weights must remain private not just from the patient but from the evaluator as well; (3) computation must be verifiable without re-running it; or (4) the use case benefits from public, decentralised access without institutional infrastructure. These conditions commonly arise in genomic research consortia, cross-institutional data sharing, and commercial PRS services.

### 9.2 Limitations and Open Problems

**SNP count ceiling.** In our mock-coprocessor measurements (Section 7), the HCU budget of 60–74 FHE operations per transaction limits each compute chunk to 20 SNPs. Scaling to genome-wide models (>50,000 SNPs) would require thousands of transactions, making on-chain costs prohibitive at any current gas pricing. HEPRS remains the appropriate tool at that scale. Future FHE coprocessor improvements may raise this ceiling.

**SNP provenance.** The system verifies ACL access to a registered sample but cannot verify that submitted encrypted SNP values faithfully represent that sample’s genotype. A malicious requester could submit arbitrary ciphertexts. Rate limiting and noisy classification mitigate information leakage per query but do not prevent fabricated queries.

**URI observability.** Sample data URIs are on-chain plaintext. Any network node can observe storage slots directly, even if read access is ACL-gated at the application layer. Storing only a cryptographic commitment to the URI would address this residual exposure.

**DP bias.** Uniform noise on  $[0, B)$  introduces an expected upward bias of  $B/2$ . True zero-mean DP would require signed noise, which the current fhEVM does not natively support. Threshold adjustment is a correctable workaround but adds complexity for deployers.

**Gas cost at L1 pricing.** Commercial viability requires a purpose-built FHE rollup or application chain. At Ethereum L1 gas prices, any SNP count is economically indefensible for routine clinical use.

### 9.3 Future Directions

Planned extensions include: (1) LD-aware weighting in the encrypted domain, incorporating LDpred2-style shrinkage [Privé et al., 2020]; (2) multi-party key generation enabling federated cohort analyses without a single decryption authority; (3) model versioning and deprecation mechanisms; (4) SNP handle re-use across multiple models from the same registered sample; and (5) token-based fee mechanisms to economically incentivise model quality. The architecture’s modularity—four independently upgradeable contracts—is designed to accommodate these extensions without disrupting existing deployments.

## 10 RELATED WORK

Privacy-preserving genomic computation has been pursued through multiple cryptographic paradigms. Kim and Lauter [Kim and Lauter, 2015] applied homomorphic encryption schemes to compute GWAS statistics for up to 5,000 sequences, but did not extend to PRS computation. Blatt et al. [Blatt et al., 2020] built a CKKS-based privacy-preserving GWAS pipeline for large-scale studies, noting that PRS computation from decrypted summary statistics was future work. McLaren et al. [McLaren et al., 2016] demonstrated privacy-preserving genomic testing in

an HIV clinical-care model using homomorphic encryption, but did not address the full PRS pipeline. Raisaro et al. [Raisaro et al., 2019] introduced MedCo for secure, privacy-preserving exploration of distributed clinical and genomic data.

Knight et al. [Knight et al., 2026] (HEPRS) is the closest prior work, providing the first complete FHE pipeline for PRS with real clinical data. HEPRS achieves  $r > 0.999$  correlation with plaintext scores on a 110,000-SNP schizophrenia model and demonstrates practical feasibility on commodity hardware. bioETH-PRS builds directly on the HEPRS computational framework and uses the same GWAS fixture datasets, extending it to a blockchain setting that removes the designated evaluator.

On the blockchain side, prior work on privacy-preserving smart contracts has focused on anonymous payments and related protocol work [Ben-Sasson et al., 2014, Pertsev et al., 2019] and zero-knowledge proof-based computation [Ben-Sasson et al., 2018], which enable verifiable computation but not confidential computation, ZK-SNARKs prove knowledge without concealing the program inputs. FHE on the blockchain, typified by the fhEVM framework [Zama, 2024], enables both confidentiality and verifiability in a single system. To our knowledge, bioETH-PRS is the first application of fhEVM to clinical genomics.

## 11 CONCLUSION

We presented bioETH-PRS, a protocol for confidential polygenic risk scoring using TFHE-based fully homomorphic encryption on a programmable blockchain. By replacing the centralised evaluator of HEPRS [Knight et al., 2026] with immutable, consensus-enforced smart contracts, we remove the designated evaluator assumption that is the principal residual vulnerability of prior centralised FHE approaches to genomic computation, while still depending on the fhEVM stack, contract correctness, ACL/decryption infrastructure, and blockchain liveness.

Key contributions are: a four-layer contract architecture with independently auditable trust boundaries; a provably overflow-safe three-step fixed-point quantisation scheme achieving machine-epsilon reconstruction accuracy on real GWAS datasets; a streaming execution path reducing on-chain gas consumption by 37%; and an on-chain noisy output oracle with cryptographically generated noise, mandatory activation, and anti-probing rate limiting.

Prototype evaluation on HEPRS fixtures confirms linear gas scaling and exact score correctness. Under L2-equivalent gas pricing assumptions, projected costs range from USD \$1.72 to \$7.95 for 100–500 SNP analyses. That range suggests the approach may be practical for curated clinical PRS panels in low-gas environments, while offering stronger evaluator minimisation than centralised alternatives.

The system demonstrates that, for the 100–5,000 SNP range covering a subset of curated polygenic models, on-chain FHE computation without a trusted evaluator is

technically feasible and may become economically practical on specialised low-gas networks. Continued improvements in FHE coprocessor throughput and purpose-built chain gas pricing will expand this range toward genome-wide models and bring private, verifiable genomic computation within reach of routine clinical practice.

## BIOGRAPHICAL NOTE

Kimon Antonios Provas, Christos Galanopoulos, and Ilias Georgakopoulos-Soares are researchers at The University of Texas at Austin studying pharmacology, genomics, and privacy-preserving biomedical computation at the Dell Pediatric Research Institute.

## DATA AVAILABILITY STATEMENT

No new datasets were generated or analysed in this study.

## CODE AVAILABILITY STATEMENT

All relevant code and results can be found on GitHub at <https://github.com/Georgakopoulos-Soares-lab/bioETH-PRS>.

## REFERENCES

- E. Ben-Sasson, A. Chiesa, C. Garman, M. Green, I. Miers, E. Tromer, and M. Virza. Zerocash: Decentralized anonymous payments from Bitcoin. In *2014 IEEE Symposium on Security and Privacy*, pages 459–474. IEEE, 2014. doi: 10.1109/SP.2014.36.
- E. Ben-Sasson, I. Bentov, Y. Horesh, and M. Riabzev. Scalable, transparent, and post-quantum secure computational integrity. IACR Cryptology ePrint Archive, Paper 2018/046, 2018. URL <https://eprint.iacr.org/2018/046>. Accessed April 28, 2026.
- M. Blatt, A. Gusev, Y. Polyakov, K. Rohloff, and V. Vaikuntanathan. Optimized homomorphic encryption solution for secure genome-wide association studies. *BMC Medical Genomics*, 13:83, 2020. doi: 10.1186/s12920-020-0719-9.
- C. C. Chang, C. C. Chow, L. C. A. M. Tellier, S. Vattikuti, S. M. Purcell, and J. J. Lee. Second-generation PLINK: Rising to the challenge of larger and richer datasets. *GigaScience*, 4:7, 2015. doi: 10.1186/s13742-015-0047-8.
- J. H. Cheon, A. Kim, M. Kim, and Y. Song. Homomorphic encryption for arithmetic of approximate numbers. In *Advances in Cryptology – ASIACRYPT 2017*, volume 10624 of *Lecture Notes in Computer Science*, pages 409–437. Springer, 2017. doi: 10.1007/978-3-319-70694-8\_15.

- I. Chillotti, N. Gama, M. Georgieva, and M. Izabachène. TFHE: Fast fully homomorphic encryption over the torus. *Journal of Cryptology*, 33:34–91, 2020. doi: 10.1007/s00145-019-09319-x.
- Y. Erlich and A. Narayanan. Routes for breaching and protecting genetic privacy. *Nature Reviews Genetics*, 15:409–421, 2014. doi: 10.1038/nrg3723.
- M. Fredrikson, S. Jha, and T. Ristenpart. Model inversion attacks that exploit confidence information and basic countermeasures. In *Proceedings of the 22nd ACM SIGSAC Conference on Computer and Communications Security*, pages 1322–1333. ACM, 2015. doi: 10.1145/2810103.2813677.
- M. Gymrek, A. L. McGuire, D. Golan, E. Halperin, and Y. Erlich. Identifying personal genomes by surname inference. *Science*, 339(6117):321–324, 2013. doi: 10.1126/science.1229566.
- M. Inouye, G. Abraham, C. P. Nelson, A. M. Wood, M. J. Sweeting, F. Dudbridge, F. Y. Lai, S. Kaptoge, M. Brozynska, T. Wang, S. Ye, T. R. Webb, M. K. Rutter, I. Tzoulaki, R. S. Patel, R. J. F. Loos, B. Keavney, H. Hemingway, J. Thompson, H. Watkins, P. Deloukas, E. D. Angelantonio, A. S. Butterworth, J. Danesh, N. J. Samani, and UK Biobank CardioMetabolic Consortium CHD Working Group. Genomic risk prediction of coronary artery disease in 480,000 adults: Implications for primary prevention. *Journal of the American College of Cardiology*, 72(16):1883–1893, 2018. doi: 10.1016/j.jacc.2018.07.079.
- M. Kim and K. Lauter. Private genome analysis through homomorphic encryption. *BMC Medical Informatics and Decision Making*, 15(Suppl 5):S3, 2015. doi: 10.1186/1472-6947-15-S5-S3.
- E. Knight, J. Li, M. Jensen, I. Yolou, C. Kockan, and M. Gerstein. Homomorphic encryption enables privacy preserving polygenic risk scores. *Cell Reports Methods*, 6:101271, 2026. doi: 10.1016/j.crmeth.2025.101271. Open Access.
- S. A. Lambert, L. Gil, S. Jupp, S. C. Ritchie, Y. Xu, A. Buniello, A. McMahon, G. Abraham, M. Chapman, H. Parkinson, J. Danesh, J. A. C. MacArthur, and M. Inouye. The polygenic score catalog as an open database for reproducibility and systematic evaluation. *Nature Genetics*, 53:420–425, 2021. doi: 10.1038/s41588-021-00783-5.
- P. J. McLaren, J. L. Raisaro, M. Aouri, M. Rotger, E. Ayday, I. Bartha, M. B. Delgado, Y. Vallet, H. F. G"unthard, M. Cavassini, H. Furrer, T. Doco-Lecompte, C. Marzolini, P. Schmid, C. D. Benedetto, L. A. Decosterd, J. Fellay, J.-P. Hubaux, and A. Telenti. Privacy-preserving genomic testing in the clinic: A model using HIV treatment. *Genetics in Medicine*, 18(8):814–822, 2016. doi: 10.1038/gim.2015.167.
- A. Pertsev, R. Semenov, and R. Storm. Tornado cash privacy solution. Whitepaper, version 1.4, 2019. URL [https://tornado.cash/audits/TornadoCash\\_whitepaper\\_v1.4.pdf](https://tornado.cash/audits/TornadoCash_whitepaper_v1.4.pdf).
- F. Privé, J. Arbel, and B. J. Vilhjálmsson. LDpred2: Better, faster, stronger. *Bioinformatics*, 36(22-23):5424–5431, 2020. doi: 10.1093/bioinformatics/btaa1029.
- J. L. Raisaro, J. R. Troncoso-Pastoriza, M. Misbach, J. S. Sousa, S. Pradervand, E. Missiaglia, O. Michielin, B. Ford, and J.-P. Hubaux. MedCo: Enabling secure and privacy-preserving exploration of distributed clinical and genomic data. *IEEE/ACM Transactions on Computational Biology and Bioinformatics*, 16(4):1328–1341, 2019. doi: 10.1109/TCBB.2018.2854776.
- Tune Insight SA. Lattigo: Lattice-based multiparty homomorphic encryption library in go. GitHub, 2022. URL <https://github.com/tuneinsight/lattigo/releases/tag/v4.1.0>. Version 4.1.0. Accessed April 28, 2026.
- N. R. Wray, T. Lin, J. Austin, J. J. McGrath, I. B. Hickie, G. K. Murray, and P. M. Visscher. From basic science to clinical application of polygenic risk scores: A primer. *JAMA Psychiatry*, 78(1):101–109, 2021. doi: 10.1001/jamapsychiatry.2020.3049.
- Zama. Confidential EVM smart contracts using fully homomorphic encryption. White paper/software documentation, 2024. URL <https://github.com/zama-ai/fhevm-solidity>. Accessed April 28, 2026.